

Dykes and structures of the NE rift of Tenerife, Canary Islands: a record of stabilisation and destabilisation of ocean island rift zones

A. Delcamp · V. R. Troll · B. van Wyk de Vries ·
J. C. Carracedo · M. S. Petronis · F. J. Pérez-Torrado ·
F. M. Deegan

Received: 14 May 2011 / Accepted: 12 January 2012 / Published online: 14 March 2012
© Springer-Verlag 2012

Abstract Many oceanic island rift zones are associated with lateral sector collapses, and several models have been proposed to explain this link. The North–East Rift Zone (NERZ) of Tenerife Island, Spain offers an opportunity to explore this relationship, as three successive collapses are located on both sides of the rift. We have carried out a systematic and detailed mapping campaign on the rift zone, including analysis of about 400 dykes. We recorded dyke

morphology, thickness, composition, internal textural features and orientation to provide a catalogue of the characteristics of rift zone dykes. Dykes were intruded along the rift, but also radiate from several nodes along the rift and form en échelon sets along the walls of collapse scars. A striking characteristic of the dykes along the collapse scars is that they dip away from rift or embayment axes and are oblique to the collapse walls. This dyke pattern is consistent with the

Editorial responsibility: M. Manga

Electronic supplementary material The online version of this article (doi:10.1007/s00445-012-0577-1) contains supplementary material, which is available to authorized users.

A. Delcamp · V. R. Troll · F. M. Deegan
Department of Geology, Museum Building,
Trinity College Dublin,
Dublin 2, Ireland

V. R. Troll
e-mail: Valentin.Troll@geo.uu.se

F. M. Deegan
e-mail: Frances.Deegan@geo.uu.se

B. van Wyk de Vries
Laboratoire Magmas et Volcans CNRS-UMR 6524, Université
Blaise Pascal, Laboratoire Magmas et Volcans, LMV, CNRS,
UMR 6524, IRD R163,
5 rue Kessler,
63038, Clermont-Ferrand, France
e-mail: b.vanwyk@opgc.univ-bpclermont.fr

J. C. Carracedo · F. J. Pérez-Torrado
GEOVOL, Dpto. Física,
Universidad de Las Palmas de Gran Canaria,
Las Palmas, Spain

J. C. Carracedo
e-mail: jcarracedo@proyinv.es

F. J. Pérez-Torrado
e-mail: fperez@dfis.ulpgc.es

M. S. Petronis
Environmental Geology Natural Resource Management
Department, New Mexico Highlands University,
Las Vegas, NM 87 701, USA
e-mail: mspetro@nmhu.edu

Present Address:
A. Delcamp (✉)
Department of Geography, Vrije Universiteit Brussel,
Brussels, Belgium
e-mail: delcampa@tcd.ie

Present Address:
V. R. Troll · F. M. Deegan
Department of Earth Sciences,
CEMPEG, Section for Mineralogy, Petrology and Tectonics,
Uppsala University,
75236, Uppsala, Sweden

lateral spreading of the sectors long before the collapse events. The slump sides would create the necessary strike-slip movement to promote en échelon dyke patterns. The spreading flank would probably involve a basal decollement. Lateral flank spreading could have been generated by the intense intrusive activity along the rift but sectorial spreading in turn focused intrusive activity and allowed the development of deep intra-volcanic intrusive complexes. With continued magma supply, spreading caused temporary stabilisation of the rift by reducing slopes and relaxing stress. However, as magmatic intrusion persisted, a critical point was reached, beyond which further intrusion led to large-scale flank failure and sector collapse. During the early stages of growth, the rift could have been influenced by regional stress/strain fields and by pre-existing oceanic structures, but its later and mature development probably depended largely on the local volcanic and magmatic stress/strain fields that are effectively controlled by the rift zone growth, the intrusive complex development, the flank creep, the speed of flank deformation and the associated changes in topography. Using different approaches, a similar rift evolution has been proposed in volcanic oceanic islands elsewhere, showing that this model likely reflects a general and widespread process. This study, however, shows that the idea that dykes orient simply parallel to the rift or to the collapse scar walls is too simple; instead, a dynamic interplay between external factors (e.g. collapse, erosion) and internal forces (e.g. intrusions) is envisaged. This model thus provides a geological framework to understand the evolution of the NERZ and may help to predict developments in similar oceanic volcanoes elsewhere.

Keywords Oceanic island rift zones · Lateral collapses · Intrusive complex · Dykes · Lateral flank spreading · Tenerife

Introduction

Oceanic islands, such as those in the Hawaiian, the Canary archipelagos, Madeira, Cape Verde or La Réunion, often show volcanic alignments associated with intense intrusive activity, known as volcanic rift zones. These structures, sometimes organised in triple-armed patterns, are often associated with major lateral collapse structures (e.g. McFarlane and Ridley 1968; Walker 1992; Carracedo 1994, 1996; Elsworth and Day 1999; Walter and Troll 2003; Hildenbrand et al. 2004; Klügel et al. 2005; Carter et al. 2007). Several models have been established to explain the observed structure and orientations of rift zones and to clarify the intimate link between rift zones and lateral collapses.

The gelatine models of Fiske and Jackson (1972) indicated that the orientations of oceanic island rift zones are topographically and gravity-controlled. The intense

intrusive activity along a rift induces forces along the flank that can eventually lead to collapse (Dieterich 1988). Carracedo (1994) proposed that triple-armed fractures are produced following doming of the oceanic crust caused by magma underplating (e.g. a plume). The rift zones will then follow these crustal triple-armed structures and instabilities in between each of the rift arms will lead to collapse. To Walker (1992), rift zone organisation and orientation are due to the structural changes induced by dyke intrusions, i.e. it is the shallow intrusions themselves that exert a control on overall swarm geometry. Volcano spreading has also been proposed as a mechanism responsible for rift zone orientation (van Bemmelen 1949; Borgia 1994; Delcamp et al. 2011) and may be coupled with volcano buttressing (Walter et al. 2006). Similarly, Klügel et al. (2005) proposed that gravitational spreading is a dominant factor controlling the volcanic rift zones and flank stability. Using gelatine-cone models and an implemented sector instability, Walter and Troll (2003) showed that an intrusion at the boundary between an unstable and a stable sector will propagate and form rift zones organised in a triple-armed fashion. Walter et al. (2005) and Acocella and Tibaldi (2005) proposed that the early stage of ocean island rift zones may be dominated by a linear geometry. Once affected by the collapse of one sector, the rift will reorganise and wrap around the collapse scar and form a third passive rift arm that will open opposite to the collapse embayment, allowing the formation of the weaker third arm of a triple-armed rift system.

With the different models proposed, it remains unclear if it is the intense intrusive activity or the collapses that actually control the structural evolution and geometry of oceanic rift zones (e.g. Dieterich 1988; Carracedo 1996; Elsworth and Voight 1996; Walter and Troll 2003). Here, we further explore the link between rift zones and collapses using field data collected along the North–East Rift Zone (NERZ) of Tenerife, Canary Islands, Spain (Fig. 1). The important result of this study is that, along collapse scars, the orientation of dykes is oblique to the walls, as observed in other collapse sectors (e.g. Tibaldi 2001; Bonali et al. 2011). This contrasts with other work that report dykes mainly parallel to scar walls (e.g. Walter and Troll 2003; Acocella and Neri 2009). We interpret such geometry (i.e. dykes oblique to the walls) as a consequence of strike-slip movements that occurred along the potential boundaries of the future collapse. Such displacements are most simply interpreted as slumping or flank spreading (van Wyk de Vries et al. 2001) that accommodated the emplacement and growth of the intrusive complex as well as the numerous multi-directional dyke and sheet intrusions (c.f. Dieterich 1988). The spreading process initially stabilises the rift by reducing the slopes and by relaxing the dyke-related stress, until with further intrusive growth, a critical point is reached

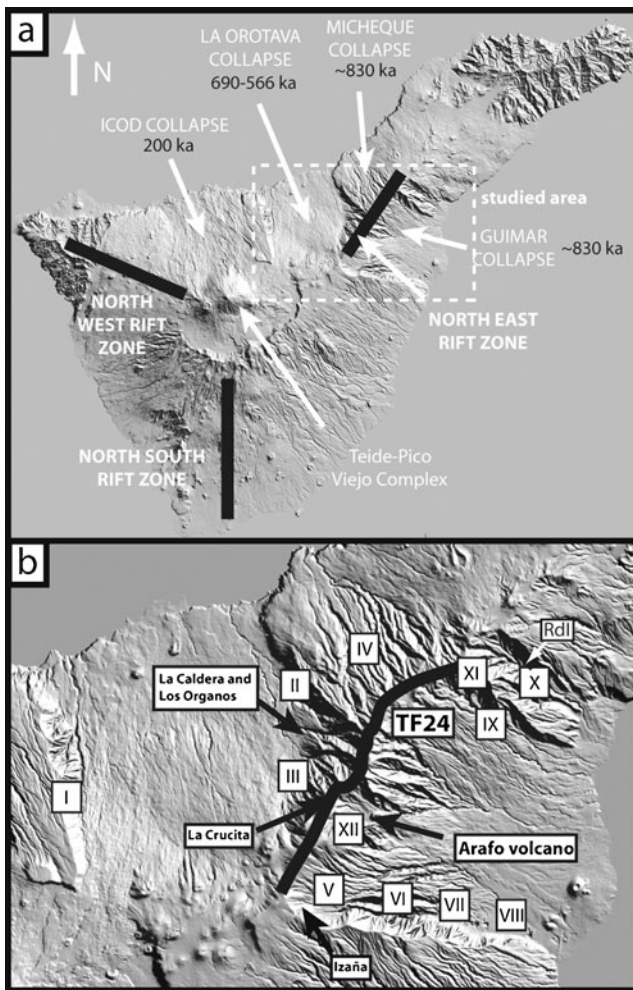


Fig. 1 **a** Shaded relief image from DEM of Tenerife (source: Grafcan©). **b** The sectors studied in this work. Sectors *I*, *II* and *III* correspond to the walls of La Orotava collapse, sector *IV* is located inside the Micheque collapse, sectors *V*, *VI*, *VII*, *VIII*, *IX*, *X* and *XI* are along the Güimar collapse scar, and sector *XII* and the road *TF24* are at the ridge of the rift zone. The galeria Rio de Igueste (*RdI*) is in sector *VI*

where new intrusions (growth of intrusive complex or dyke–sill emplacement) will generate collapse. Using field data, we propose a dynamic model for the evolution of the NERZ that differs from the widely held view of oceanic rift zones being simple parallel arrangements of fractures, dykes, and volcanoes (e.g. Acocella and Neri 2009) or that they merely reflect main oceanic crust or plume-related fractures (e.g. Geyer and Martí 2010).

The study area

The geology of Tenerife is a matter of lively debate within the scientific community. Here, we present a brief summary of what is commonly accepted. Three successive Miocene–Pliocene shield volcanoes (Roque Del Conde, Anaga and Teno) represent the early stages of Tenerife Island (Fúster et al. 1968; Ancochea et al. 1990; Guillou et al. 2004; Carracedo et al. 2007; Longpré

et al. 2008). Following a gap of two to three million years, a major central volcano, Las Cañadas, built up (Ancochea et al. 1990; Martí et al. 1994; Carracedo et al. 2007). Volcanic eruption persisted (~2–0.5 Ma), until a major lateral collapse occurred at ~200 ka, forming the Las Cañadas caldera (c.f. Watts and Masson 1995; Martí et al. 1997; Martí and Gudmundsson 2000; Carracedo et al. 2007). Following this major event, the Teide–Pico Viejo stratocone started to form. In parallel to the evolved Las Cañadas and the Teide–Pico Viejo complex, extensive basaltic activity also occurred along the rift zones (Ancochea et al. 1990; Carracedo et al. 2007).

Tenerife is composed by three main rift arms (North–South, North–West and North–East) with major collapses embayment in between these. The NERZ, orientated 040°, displays the best outcrops among the three rifts and has thus been chosen to further investigate the link between intrusion and collapse. Also, three successive collapses (1—Micheque, 2—Güimar, 3—La Orotava) are located on the two sides of this rift. Recent work by Carracedo et al. (2010a) showed that the NERZ is characterised by three main stages of volcanic activity: a Miocene (7.203 Ma ±155 ka), a Late Pliocene (2.710 Ma ±58 ka) and the latest one during the Pleistocene. Each volcanic stage seems to be intense and relatively short-lived (few hundred thousand years) compared with the lifetime of the entire volcano. During the Pleistocene, three major collapse events affected the NERZ, commencing at about 830 ka, a sector on the north of the rift collapsed, forming the Micheque embayment. Shortly afterwards (around 830 ka as well), another collapse occurred on the south–east flank of the rift, producing the Güimar landslide embayment. The last collapse, La Orotava, affected the north side of the rift and is estimated to have occurred between 690 and 566 ka, partly affecting portions of the former Micheque landslide fill. At present, the Micheque embayment is almost completely obscured by post-collapse volcanism, while Güimar and La Orotava have only been partially filled.

Methodology

We divided the NERZ into 12 sectors (labelled from *I* to *XII*; Fig. 1b) in which the dyke lithology, structural textures, orientations and shapes were recorded. Country rock lithology and structure was also noted. Sectors *I*, *II* and *III* correspond to the walls of La Orotava collapse, sector *IV* is located inside the Micheque collapse, sectors *V*, *VI*, *VII*, *VIII*, *IX*, *X* and *XI* are along the Güimar collapse scar and sector *XII* along the road *TF24* is on the ridge of the rift zone. We also visited two galerias (water tunnels): Aguas de San José at about 1,130 m a.s.l. in sector *VII* along the SW Güimar collapse scar and Rio de Igueste (*RdI* on Fig. 1b) at 400 m a.s.l. in sector *X* along the NE scar of Güimar. After a brief description of the petrography and composition of the dykes, we

will describe the various dyke morphologies followed by the structural data.

Field observations

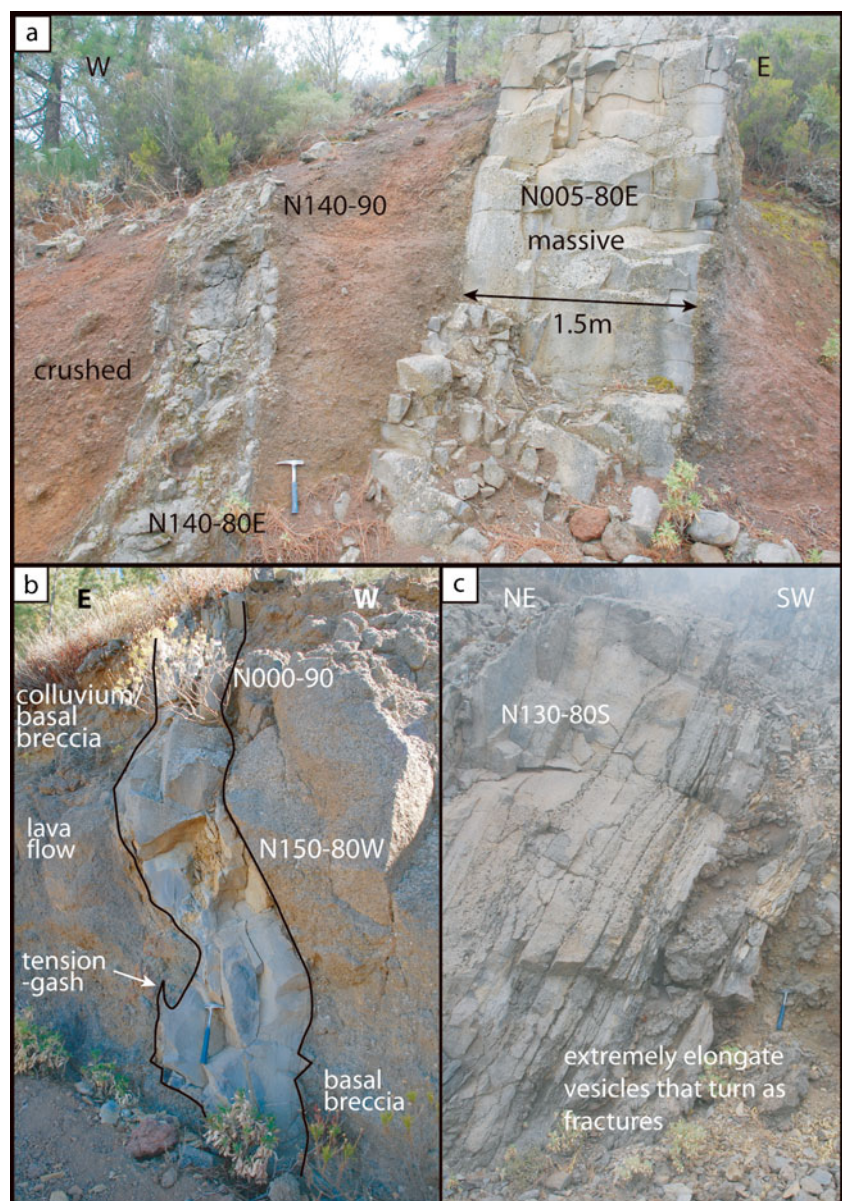
Dyke petrography and composition

Using hand samples and thin sections, we identified classical rock-forming minerals such as olivine, pyroxene and plagioclase, which allowed us to distinguish six petrographic groups: the most abundant one is the aphyric group, then the second group is plagioclase-rich, the third group is plagioclase- and clinopyroxene-rich, the fourth group is ankaramitic, the fifth group is olivine- and clinopyroxene-

rich and the last group is pyroxene-rich. More details on dyke petrography and dyke groupings can be found in the [Electronic Supplementary Material](#).

On a TAS diagram (Le Maitre et al. 1989), most of the dykes fall into the basanite field with a few plotting in the basaltic trachyandesite, trachyandesite, tephriphonolite and phonotephrite fields (see Fig. 2 of the [Electronic Supplementary Material](#)). No clear correlation between the petrographic, geographic and compositional groupings has been identified (Delcamp et al. 2010). In this paper, we shall use the compiled data mainly for classification, whereas magma source and differentiation processes will be the focus of a separate study. The petrography and composition of the dykes indicate that substantial magma differentiation has occurred within the rift (Deegan 2010).

Fig. 2 Examples of dyke morphologies and textures. **a** Example of representative massive and crushed dyke, **b** example of dyke with gently deviating strike. Note the dyke injection formed a tension gash within the country rock, **c** example of dyke containing vesicles; in this case, the vesicles are concentrated in bands parallel to the margins and they start to form fracture-like parallel joints



Dyke descriptions

Dyke diversity and morphology

Here, we present a brief overview on dyke morphologies and dyke internal structures. More detailed descriptions and figures can be found in the [Electronic Supplementary Material](#). The dyke morphology is diverse, ranging from massive to intensely fractured or crushed, from highly vesicular to low vesicularity and from straight to bendy (Fig. 2). Orientations of individual dykes are usually constant at the outcrop scale, but local changes in strike, in dip or both have sometimes been observed (Fig. 2a, b). Changes in orientation (strike, dip or both) can occur at the boundary between layers of different competence, such as between a lava flow and its basal breccia, but occurs also within the same layer (e.g. Hoek 1995; Gudmundsson 2002).

Vesicle shapes and sizes are also variable. An interesting feature to note is that sometimes vesicles concentrate along straight bands parallel to dyke margins and, when their number and size becomes significant, they form fracture-like parallel structures within the dykes (Fig. 2c). In such cases, vesicles are elongate, stretched and often ruptured.

A few dykes contain centimetre-sized xenoliths of local country rock. Short finger-like intrusions into the adjacent rocks are sometimes observed (Fig. 2b), similar to those described by e.g. Mathieu and van Wyk de Vries (2009). These intrusive fingers may be tension gash-like features or dyke tip branching relics.

Dyke thickness and density

The average of all dyke thicknesses for the entire study area is 128 cm (Fig. 1, $N=531$ dykes). Dyke thicknesses for each sector (Fig. 1b) are displayed in Table 1 and were calculated as follows: when only an estimate of a dyke's thicknesses

was available, i.e. dykes observed from a distance, the values were not taken into account for the calculation. Within a dyke, thickness variations can occur, especially when the dyke passes from a low competence zone (e.g. scoria) into a more resistant stratum (e.g. a lava flow) where the dyke becomes thinner (see the [Electronic Supplementary Material](#)). If a dyke was accessible and measurable with a tape measure, then the thickest part of the dyke was considered. Some of the thicknesses estimated along trail VII from afar were still used for the calculations of means since insufficient direct measurement were available from this sector. This track cuts steep cliffs that cannot always be safely approached, but view points were sufficiently close to get reasonable estimates of the true dyke thicknesses. Figure 3a shows the overall distribution of dyke thickness. Most of the dykes are between 31 and 60 cm thick. Note that the average dyke thickness (128 cm) is shifted from the highest frequency peak (i.e. 31–60 cm) and we observe a progressive decrease in frequency towards larger thickness values.

As shown in Table 1 and Fig. 3b, dykes at higher and at intermediate altitudes are generally thinner than those at the base of the ridge. Moreover, in La Crucita (LC in Table 1—belonging to sector III, see Fig. 1b), two dykes of 10 m thickness were found. If these are not included for the La Crucita average calculation, the result changes from 265 to 118 cm (denoted by an asterisk in Table 1). One of the trails in sector VI leads down into the Güímar valley where a dyke swarm can be observed. From a distance (~between 100 and 150 m), the dykes were estimated to be between 1 and 2 m in thickness.

We evaluated the intrusive density by adding the thicknesses of all the dykes along a measured cross section. Where thickness variation occurred, the average was taken into account. The dyke density is generally higher towards the ridge axis and along the SW and NE side of the Güímar scar. No dykes have been found along the west side of La Orotava

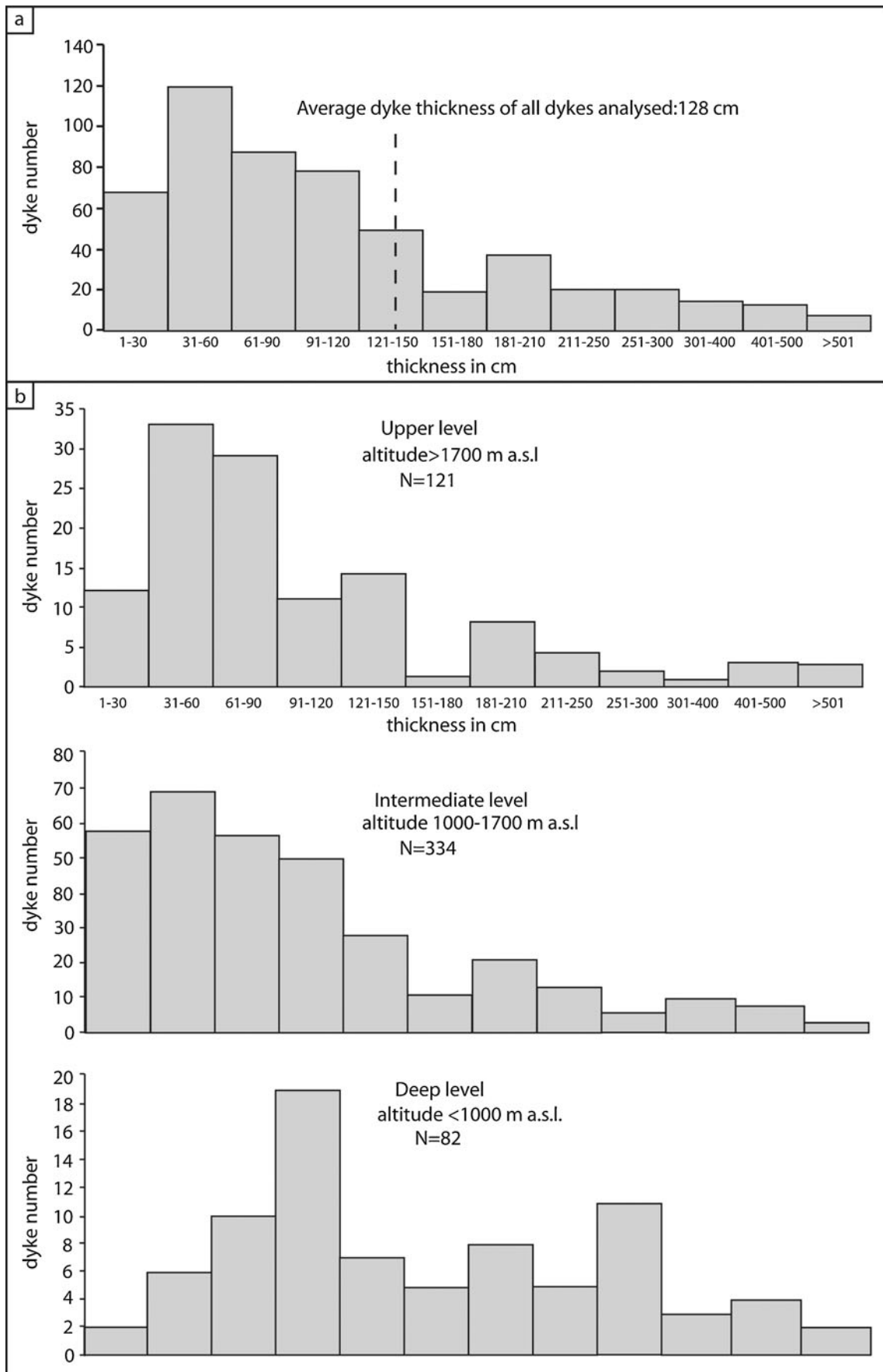
Table 1 Average dyke thicknesses for each sector (Fig. 1b)

Sector	Road TF24	I/II/VIII	III	IV	V	VI	VII	IX	X	XI	LC	RdI
Dyke number (N)	98	0	45	74	12	62	30	9	6	131	12	52
Average dyke thickness (cm)	105	/	188	91	72	82	120	149	93	116	265/118*	246
Minimum value of dyke thickness (cm)	15	/	24	10	30	1	30	10	40	3	30	10
Maximum value of dyke thickness (cm)	650	/	1,200	460	150	270	300	300	200	550	1,000	1,600
Standard deviation (SD)	78	/	119	58	40	63	108	91	58	77	/	175
Average–SD	39	/	47	22	/	26	67	/	/	27	/	72
Average+SD	161	/	5,553	153	/	152	172	/	/	217	/	422

Units are in centimetres. The thicknesses follow usually a normal distribution. Thus, the SDs were calculated from the logarithm of the thickness values. The distributions of dyke thicknesses in sectors V, IX and X follow a Gaussian curve, allowing SD to be calculated from the data. For La Crucita, the distribution follows neither a Gaussian curve nor a normal law. Note that the SDs are of high values as the range of thickness is large (see minimum and maximum values)

LC La Crucita (belong to sector III), RdI Rio de Igueste

*see text for explanation



◀ **Fig. 3 a** Histogram showing dyke thickness distribution (in centimetres). Number of dykes for each thickness category is displayed on the y-axis. Most of the dykes plot in the 31–60 cm category. **b** Histograms representing the number of dykes for each thickness category (in centimetres) for a specific altitude interval. Note that the horizontal axes are the same for the three altitudes. From *top* to *bottom* altitude >1,700 m (highest), altitude between 1,000 and 1,700 m (intermediate) and altitude <1,000 m (lowest). Dykes are generally thicker at lower altitudes

valley. The east side of the La Orotava scar is mainly covered by vegetation and a thick pine needle cover that hide outcrops.

Intrusive densities were also calculated from three different portions along the road TF24, i.e. the upper part of the rift (Fig. 1b). The three considered portions of 437, 119 and 283 m give intrusive densities of 2.6%, 3.6% and 9.9%, respectively. The average intrusive density for these three horizontal logs is 5.2%. For sector X, an intrusive density of 5.7% along a section of 1.7 km and of 6.6% along a 2.3-km

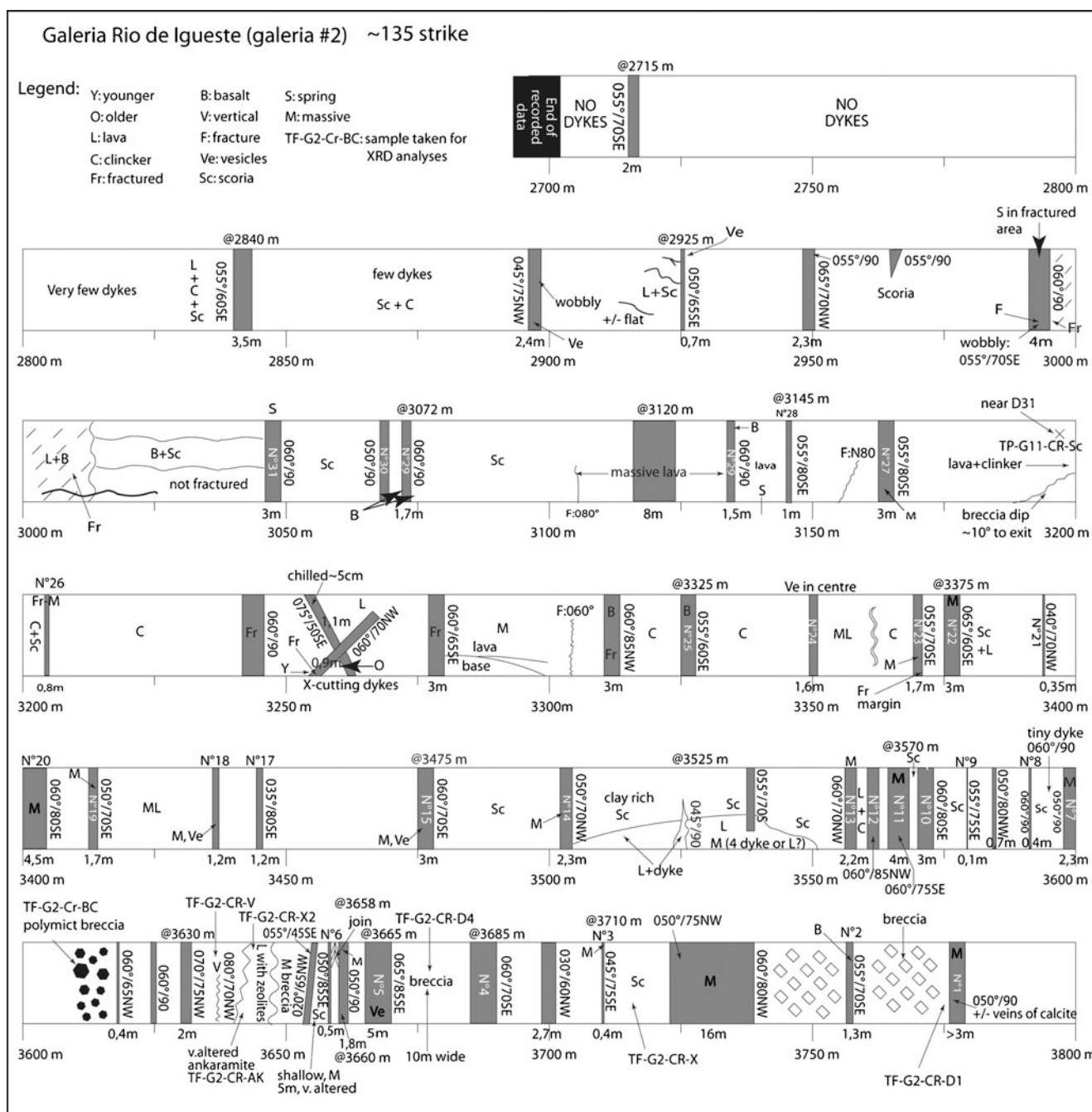


Fig. 4 Cross section of the galeria Rio de Igueste orientated 135°. The symbol key is shown on the *top left corner*. Dykes are represented by *grey rectangles*

section has been calculated. Sector III is at an intermediate altitude relative to the galerias (water tunnels which are the lowest accessible part of the rift). In sector III, the intrusive density is 2.4%. In the galeria Rio de Igueste (Fig. 4; sector X), the intrusive density calculated along a 1.08-km section is 11.8%. However, if the last 800 m of the galeria is considered in isolation (the portion closer to the rift axis), the intrusive density increases to about 14%. For sector XII, a value of 4.6% along a 775-m section is derived (see Table 2).

Country rock

The dykes intrude mainly lava flows and their associated basal and top breccias and lapilli and scoria deposits. Up on the rift, along the road TF24, several dykes intrude colluvial deposits, which underline the existence of paleovalleys and considerable local erosion and reworking even during rift growth.

In several places across the study area, crushed lava flows have been observed, which resemble crush zones within fault planes. Sometimes, these lava flows are turned into a fine white to grey powder. This could be due to intense post-emplacement deformation and/or intense alteration.

Compared to massive lava flows or massive units, such brecciated and altered layers will have lower tensile strength and cohesion and may flow by ductile deformation (e.g. Rodríguez-Losada et al. 2009). Such layers are widely referred to as low strength layers (cf. Oehler et al. 2005).

The galerias are a humid environment where the rocks are very crumbly and in places strongly weathered due to interaction with water. Dykes are intruded into fractured lava and unconsolidated or semi-consolidated scoria (Fig. 4). Several localised and strongly fractured zones with chloritised surfaces were identified, but with overall low dips. Clays have not been detected in appreciable amounts in samples of lava flows and scoria using X-ray diffraction (Delcamp 2010), but if these rocks experience a high lithostatic pressure (i.e. when situated at a deep level), they are likely to offer limited resistance to deformation and may act as low strength layers at depth.

Structural observations

Only few cross-cutting relationships between dykes have been observed and these are insufficient to infer relative ages between different dyke populations. Rose diagrams for each sector (Figs. 1b and 5) have been constructed, using only data (strike and dip) we could measure directly with the compass. Estimates from afar, typically dyke swarms, are reported

in grey for information, but are not taken into account for the final model as they are not precise. Where strike variations occurred, we took the averaged direction, but only if the deviation was less than or equal to 30°. If the deviation was more than 30°, directions were not averaged and were not plotted in the rose diagrams (17 dykes). Where dip variations occurred, we took the average into consideration. In this way, we aim to establish the main volcano-tectonic trends.

The distribution of dykes and structures is given in detail in the additional material. Here, we summarise the general trends. The dykes along the ridge axis tend to be parallel to this axis, with various dip. The dykes outside the ridge generally dip outward, i.e. the dykes that are at the north, west and north-west of the ridge dip to the north, west or north-west, and reciprocally, the dykes at the south, east and south-east of the ridge dip to the south, east and south-east. In the collapse scar and along the scar side, there is an important deviation from the ridge trend where dykes are found en échelon and strike oblique to the scar wall. This is particularly clear to the south side of the Guimar valley (c–e on Figs. 5 and 6), but is also observed on the Guimar north side (f and g on Figs. 5 and 6). On Micheque, few dykes strike E–W and could have been related to sliding on the Micheque embayment. On La Orotava, several dykes are highly oblique to the walls and could relate to La Orotava slumping. The overall pattern is a main rift trend with dykes forming arcs that cut oblique to the collapse scar walls (Fig. 7).

Field interpretations

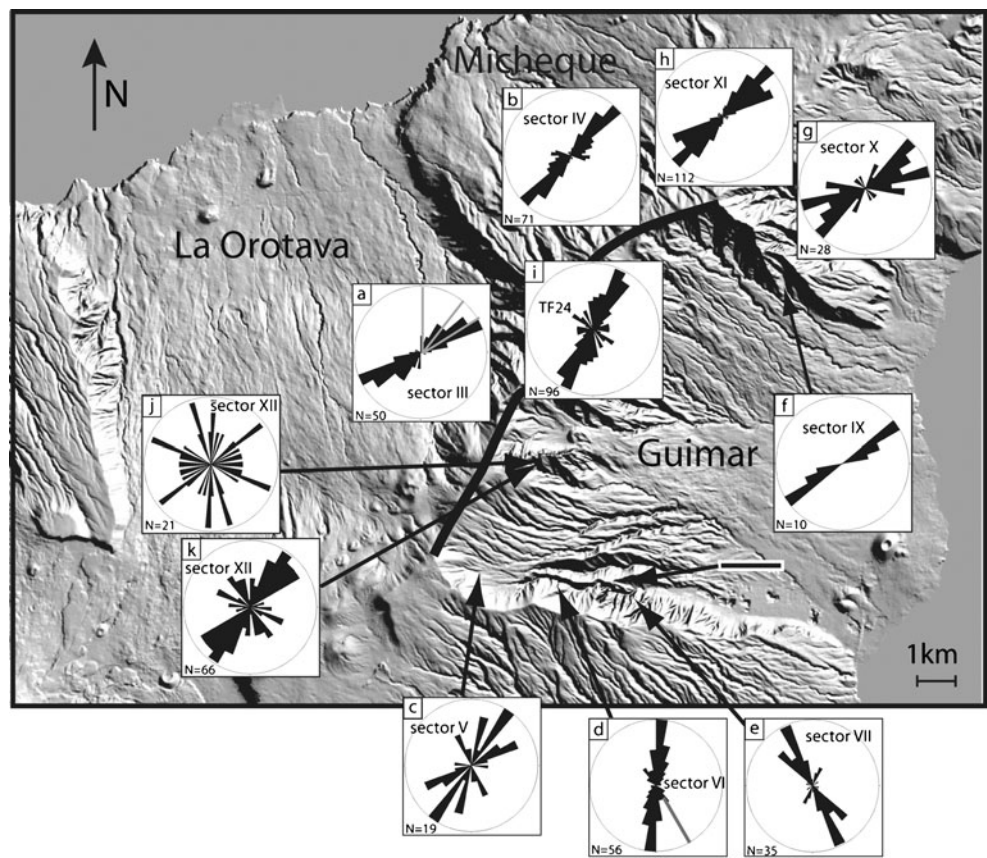
Vesicle distributions and fractured dykes

Mechanisms that can be envisaged for the described fractured dykes include (Fig. 2a) (a) cooling, (b) movement of magma during cooling, (c) local tectonic movement, (d) variation of Young's moduli between the dykes and host rocks (Porreca et al. 2006) or (e) a combination of these processes. Some of the dykes contain vesicles, sometimes in high concentrations, distributed along bands parallel to the dyke margins (Fig. 2c). The vesicles are usually highly stretched and interconnect to form open fractures. It can be inferred that (1) while the magma is flowing within a dyke, vesicles follow preferential paths and concentrate along straight bands parallel to the dyke margins; (2) with progressive cooling and deformation, bubbles stretch and are then

Table 2 Intrusion density calculated in several sectors (Fig. 1b)

Sector/site	Road TF24	III	VII	XI	Galeria RdI		
Section length (m)	437	119	283	3,500	775	2,300	1,080
Intrusion density (%)	2.6	4.2	9.9	2.4	4.6	6.6	11.8

Fig. 5 Rose diagrams of dyke orientations observed in the different sectors studied (Allmendinger et al. 2012). *a* Note the structural trends in grey that are observed on satellite image of the north scar of La Orotava (sector III) for comparison. *d* Dyke swarm direction measured from afar in grey. *e* Note the dyke swarm represented by a dashed grey line measured north of the scar. *j* Rose diagram of the dyke orientations that could be directly measured in sector XII. *k* Orientation of dyke swarms (distant but unambiguous measurements) in sector XII



disrupted by fractures as the material becomes brittle; (3) the temperature is still decreasing and the deformation is now brittle with full fracture formation. In addition, progressive

cooling will promote microlite growth and flow will cause alignment parallel to flow direction, creating a preferential parting direction. This is seen in many dykes and lava flows.

Fig. 6 Stereoplots of dyke poles for each sector studied, reflecting the direction of dyke dip relative to geographical position

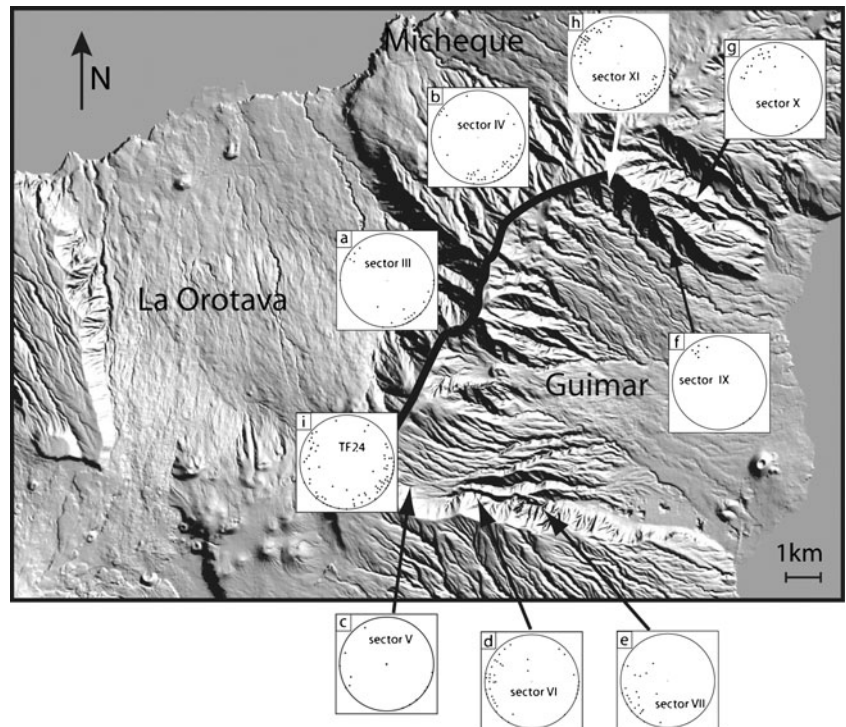
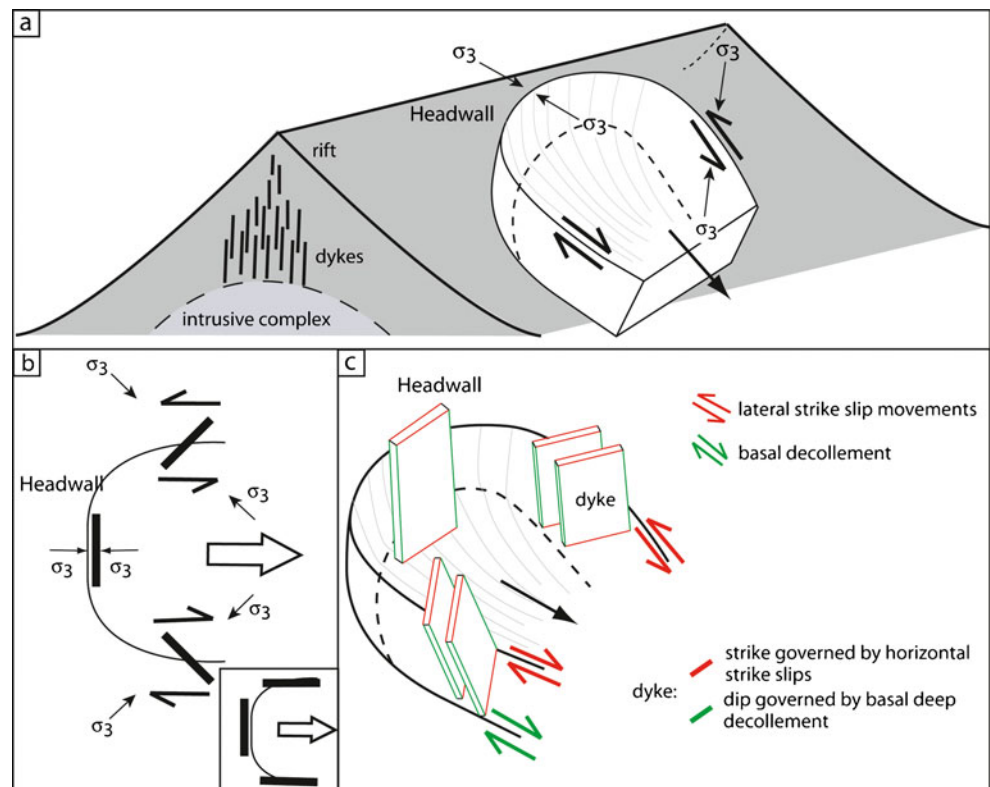


Fig. 7 Interpretative sketches of dyke orientations and geometry displayed along the collapse scars. **a** Stress field orientation and resulting displacements. **b** 2D plan view of dyke orientations resulting from the stress field displayed in **a**. Classical model of dyke orientation around a lateral collapse scar shown for comparison in the *small box* (e.g. Walter and Troll 2003; Acocella and Neri 2009). **c** Interpretative sketch showing the relation between basal- and strike-slip fault zones and the resulting dyke orientations in the upper part of the rift during pre-collapse spreading and slumping



This explanation may be valid for dykes such as the one in Fig. 2c, but intense stretching during cooling is not likely to be the only process to cause dykes to fracture. In sector XI (Boca Del Vallee), one direction of fracturing is prominent (040°) and likely represents a local volcano-tectonic trend (Fig. 3 of the [Electronic Supplementary Material](#)). This implies that this preferential volcano-tectonic direction was active during and/or after dyke cooling. Unfortunately, it is not possible to conclusively distinguish between the two fracturing origins (cooling or tectonic) and it is probable that the two acted in concert. The crushed dykes and the crushed zones within some dykes are, however, interpreted to have a volcano-tectonic origin, as cooling is not likely to be responsible for the formation of such jigsaw-like fractures (i.e. Fig. 2a).

The magma flow direction can be approximated in some dykes, when vesicles form a “V” pattern between the paired margins (see the [Electronic Supplementary Material](#)). Upward flow is inferred when the “V” pattern points upward and downward flow is implied when the “V” pattern points downward. This geometry is due to a magma velocity and shear strain gradient across a dyke (velocity increases from the margins towards the centre). The fact that the vesicle shapes and that such “V” patterns are preserved after cooling suggests that the magma had then cooled sufficiently at that point to become viscous enough to prevent bubbles from rising any further.

Dyke thickness and density

In general, a slight thickness increase of dykes towards the base of the rift is observed. The variation of dyke thickness is not significant between the upper and intermediate altitude levels, however. If, in turn, we compare the upper and intermediate levels with the deepest level (corresponding to the galeria), the thickness variation is considerably more pronounced (Fig. 3b).

Dykes are mainly concentrated along the rift and along the Güimar valley scars. Consequently, the intrusive activity seems to have been concentrated in these sectors, but not in the La Orotava area. Note that the dyke densities reported depend on the amount of outcrop found and so the true density may be somewhat higher. For example, the few older dykes and feeder dykes of recent scoria cones found at the south-west part of the rift (from the National Park entrance) are covered with lapilli and scoria deposits and it is highly probable that more dykes lie buried under the deposits. Dyke density in this locality may thus be higher. The intrusive density increases with depth (e.g. galeria Rio de Igueste) in agreement with several previous studies, which have indicated that dyke proportion is higher at deeper structural levels within the edifice as many dykes become arrested before reaching the surface (e.g. Hoek 1995; Gudmundsson et al. 1999; Gudmundsson 2002).

Country rocks

On the upper part of the rift, several dykes are surrounded by colluvium deposits, which are often gently baked due to heating associated with dyke emplacement. The dykes are thus younger than the colluvium deposits. Consequently, the upper part of the rift has experienced period(s) of erosion that were concurrent with intrusive activity.

Structural interpretation of dykes

A deviation of dyke orientation (strike, dip or both) at the transition between two layers of different resistance is likely due to local changes in the stress field induced by the difference in competence between the layers (e.g. Hoek 1995; Gudmundsson 2002). However, if the strike, dip, or both change within the same stratum, the variation is more likely due to a local stress field. The deviation can also be due to the dyke propagation mode, especially if the observed part of the dyke is close to the tip. Several observed dyke tips are distinctly “wiggly” like those modelled by Mathieu and van Wyk de Vries (2009) that show a propagation mode by viscous indentation rather than hydraulic fractures. A divergence in dyke orientation (strike, dip or both) may occur when an older dyke is close to another. In this case, the deflected dyke is likely younger.

Micheque

The Micheque collapse corresponds to sector IV (Fig. 1b). The 14 dykes recorded directly at the western side of the Micheque collapse are orientated E–W. This direction could be the result of local strike-slip movements along the sector associated with a flank creep. Further east, the dykes are orientated along a 030° to 050° trend that represents the main rift direction. Several dykes dip towards the N, W and NW, suggesting that the principal stress axes were inclined (Fig. 7a). Such a configuration can be due to local topography effects (e.g. van Wyk de Vries and Matela 1998) and/or can occur if the ridge flank spreads towards the sea and the progressive displacement along a basal decollement is accommodated by the opening of N, W and NW dipping fractures, parallel to the rift direction.

Many vertical dykes also have been recorded at the head of the collapse, suggesting a horizontal minimum stress component (σ_3) and horizontal stretching. We thus have two different minimum stress components: one tilted and one sub-horizontal. These two components are observed across the studied area. Unfortunately, it is not possible to determine their relative ages.

Güimar

The dykes in sector VI mainly trend 000°, but strike directions of 140–160° become dominant toward the south. In sector VII, the dykes mostly trend 130–150°. The majority of the dykes dip towards the E or SE. This is downslope and suggests that principal stresses are also inclined relative to the topographic free surface.

Three key observations are consistent with flank creep towards the sea: (1) the consistency of the dyke dips (E and SE), (2) the progressive change of dyke strike from the N to the S (from sector VI to VII) and (3) the fact that the dykes are not always straight, reflecting a locally variable stress field. The 000° direction found in the western part of sector VI is consistent with extension at the head of the collapse, while the NW–SE direction along the side of the collapse is consistent with strike-slip movement (Fig. 7a). The 000° trend is also found in one galeria to the north of sector VI (Carracedo et al. 2010a).

The NE side of Güimar valley is slightly more complicated than the SW. There dykes mainly dip to the E, S and SE, consistent with slow displacement (creep) along a basal decollement. The 050° direction (sectors IX and X) could either represent the rift trend or the strike-slip movement related to the creeping zone edge (Figs. 5f–h and 7b). However, sector X is outside the scar and shows another trend at 060–070°. This direction can be a deviation of the rift. The direction 070–090° is also found in sector IV (Micheque). Large deep vertical canyons are observed in the field in sectors IX and X that run approximately parallel to the scar (i.e. NW–SE with some kinks) and may correspond to major faults.

La Orotava

The dykes at the NE corner of the head of La Orotava valley (sector III) are mainly orientated along a 060° trend. A few major sets of fractures are observed, demonstrating an intense deformation at the head of the collapse. The NE–SW trend may correspond to the rift direction. The N–S and the ENE–WSW are vertical and are most simply interpreted as set of strike-slip conjugate faults. The 060° set is denser and dominant, possibly due to the proximity to the head of the landslide. Strike-slip motion is also supported by clockwise rotation inferred from paleomagnetic data (Delcamp et al. 2010).

Similarly to the head of Micheque collapse, most of the dykes are vertical or dip towards the north, west and north-west, suggesting a horizontal and an inclined stress field. However, as explained before, it is not possible to know if these stress fields acted at the same time or to give a relative age.

The ridge

The 040° direction recorded along the Boca Del Vallee trail (sector XI) most likely represents the rift orientation. No preferential direction has been observed for the dip of the dykes, though. Towards the W of this trail, we recorded vertical dykes or dykes dipping mainly towards the S and SE, as observed in sectors IX and X that are consistent with slow spreading and creep. Still at the W of the track, two main directions at 040° and 060° were recorded, with 060° being considered a deviation of the rift. The dykes observed along the road TF24 display a dominant direction towards the NE and are thus sub-parallel to the rift. However, paleomagnetic data showed that the dykes have undergone major rotation (Delcamp et al. 2010) and were thus not originally parallel to the NERZ axis. Nevertheless, a large variability in strike and dip is observed at the outcrop scale. This road is at the upper part of the rift, probably close to the old topographic surface. Thus, the variation of dyke orientation on the rift crest does not reflect any deep or regional stress field and can be explained by near-surface effects (Delaney and Pollard 1981; McGuire and Pullen 1989; Gudmundsson 2000; Tibaldi 2003; Klügel et al. 2005; Acocella and Neri 2009). Local topographic effects can also explain the strike orientation variability of the dykes recorded on the SW side of the head of Güímar valley, which intrude the Izaña cinder cone (Fig. 1b), and a portion of the dykes of sector XII, which are located at high altitude, almost at the same altitude as the ridge.

Discussion

The patterns of dykes and their orientations are indicative of the stress and strain regime in the rift over the time scales of its growth and deformation. With the absence of major regional faulting around Tenerife, internal sources of deformation need to be found (e.g. Carracedo et al. 2010b). The most significant are magmatic (dykes and their deeper intrusive complex sources) and gravitational (creep on hydrothermally altered rock, magma and low strength layers). Sea level changes and erosion could also have a role in triggering deformation although sufficient information on those phenomena is not available to judge. Flexure of the crust by loading could also have an effect (Watts 1994; Canales et al. 2000).

The fractured and crushed dykes frequently recorded in the studied area can be an indication of post-emplacment deformation, parallel to their strike, during and/or after their cooling. Using dyke orientation patterns across the NERZ, two types of deformation were inferred: (1) basal detachments responsible for an inclined σ_3 and the formation of seaward-dipping fractures and (2) accompanying local

lateral strike-slip movement responsible for a modified dyke strike, oblique to the spreading sectors, the subsequent collapse walls (Fig. 7c). It is also possible that basal decollement accommodated part of the rift extension, allowing for the coexistence of vertical and tilted dykes (Fig. 7c). Lateral strike-slip movements and basal detachments reflect a progressive and continuous deformation. Furthermore, the dykes, either at the head or along the scar walls, have various petrographic compositions (ankaramite/oceanite) and cover a large time scale of emplacement (Carracedo et al. 2010a; Delcamp et al. 2010). This suggests that dykes have intruded the rift zone during several hundreds of thousands of years and that the magmatic plumbing system remained active and evolved, allowing new compositions to be produced. Consequently, the geometries, the orientations, the range of compositions, the ages and sometimes the aspect (fractured or crushed) of dykes strongly suggest that they were emplaced during an episode of progressive, prolonged and localised flank deformation. Moreover, the available dyke emplacement ages predate the collapse events (Carracedo et al. 2010a; Delcamp et al. 2010). This is a strong argument showing that dyke's main trends do not reflect local topographic control due to later lateral collapse, but that their orientation are likely due to the slow deformation of the spreading flank. In addition, if intrusion had occurred after collapse, dykes would have intruded parallel to the scar, which seems not the case in the NERZ. We note that a few eruptions, e.g. Quaternary cones have occurred not necessarily along the collapse margins, suggesting that here the scar geometry has had a lesser effect on dyke concentration than elsewhere.

Thus, the dykes within the NERZ do not follow a simple arrangement, neither parallel to the rift axis nor parallel to the collapse scars. The oblique orientation of the dykes along the scars of the collapses contrasts widely with the observation of dykes arranged parallel to the collapse walls (e.g. Walter and Troll 2003; Walter et al. 2005; Acocella and Neri 2009; Fig. 7b). This suggests that the topography of collapse was not a key control on dyke orientation. Furthermore, paleomagnetic data have shown that dykes on the ridge (along the road TF24) have been globally rotated clockwise by 26°, meaning that the general dyke orientation before rotation was not NE–SW at the ridge and hence not parallel to the ridge axis (Delcamp et al. 2010).

The flank creep process implies a slow motion (i.e. flank spreading) of one sector of the edifice (volcano or rift) due to intense intrusive activity, for example, through spreading and inflation of the underlying intrusive complex (Dieterich 1988; Delcamp et al. 2011), probably along pre-existing low strength layers (Merle and Lénat 2003; Oehler et al. 2005; Márquez et al. 2008), such as the crushed and pulverised layers described from the field. Field observations on other rifts associated with landslides will be very helpful to test

our model and analogue models can be employed to see if features observed in the field can be reproduced in a laboratory.

Flank deformation over a long period would allow seaward-dipping fractures to form and be exploited by dykes. A similar mechanism has previously been suggested for the Anaga massif, NE of Tenerife (Walter et al. 2005). However, Walter et al. (2005) observed that the older dykes dip landwards, which is possible if the creep persists long after dyke emplacement, allowing dykes that initially dip seaward to be rotated. Furthermore, the stress field and the location of the deformation at Anaga and the NERZ are very different, representing different domains of a slide (below and above the decollement, respectively). For instance, the stress conditions below the decollement may be more strongly influenced by the intrusive complex than the stress field above the decollement. It is hence possible that the dip of the NERZ dykes below the decollement may have been rotated downslope and thus may dip landward, as in Anaga.

The dykes are slightly thicker and their density higher at the deepest part of the rift (especially in the galeria Rio de Igueste). The deformation initiated by the intrusions is thus higher at the base and favours the production of a deep decollement level. Furthermore, dyke intrusion is accompanied by an increase of pore fluid pressure that allows a decrease in the friction coefficient (frictional resistance) and thus favours failure (Elsworth and Voight 1996).

From previous work, we infer that the rift was built during three main stages of intense volcanic activity during the Miocene, the Upper Pliocene and the Pleistocene (Carracedo et al. 2010a). During these peaks of growth, the intrusive activity was high and probably semi-continuous (Carracedo et al. 2010a). As the different periods of activity were probably short (few hundred thousand years), the rift was able to progressively accommodate the intrusive core and associated dyke emplacement by flank creep. The last period of activity during the Pleistocene was more intense and the rift was not able to accommodate intrusive core growth and further dyke emplacement by flank spreading alone. Despite the rift being able to temporarily reach a semi-stable state by flank spreading, its height was increasing and its slopes were becoming oversteepened. Therefore, with each new intrusive event, the rift progressively evolved towards an unstable configuration and eventually a major lateral landslide occurred. Consequently, although the initial stage of rift construction may be controlled by a regional stress field or by pre-existing structures (Beck and Lehner 1974; Anguita and Hernán 1975; Robertson and Stillman 1979; Araña and Ortiz 1986, 1991; Carracedo 1994; Geyer and Martí 2010), progressively, however, the growing intrusive complex(es) and topographic ridge take control of the near-surface stress field in maturing rift systems (Fig. 8).

Chronology of the collapse events

The relative chronology between the different collapses deduced from stratigraphy and geochronology data by Carracedo et al. (2010a) is consistent with our structural data. In the Pleistocene phase, the rift was accommodating the growing intrusive core and dyke emplacement by flank creep that, in turn, favoured more dyke intrusions, corresponding to a positive feedback loop. The rift was becoming progressively steeper and was developing an intrusive core. A sector of the rift began to slump, modifying dyke orientations and eventually leading to the collapse that formed the Micheque embayment. Following this first mass-wasting event, the Micheque scar was rapidly filled by eruptive products. The other side of the ridge, already in an unstable state, was weakened by this major event and responded by another lateral collapse, creating the Güimar embayment. Activity of nested volcanoes continued to fill the Micheque embayment and started to fill Güimar. No dykes have been found along the scar of La Orotava collapse (except at the head). This last collapse is, therefore, probably not intrusion-driven, but largely gravity-controlled, as this part of the NERZ was severely weakened by the previous intrusion-collapse episodes. Destabilisation could have been localised on specific mechanically weak horizons, such as scoria or partially deformed lava flows as found in the field and in the galerias, or by the land–sea interface which contains weak rocks. La Orotava valley was thus probably partially formed by simple sliding on weak flank substrates.

The field data do, however, not show if one scar corresponds to one or several collapse events. We propose that different blocks slid at different rates, leading to a set of strike-slip faults and collapsing sectors, as it has been also proposed by Delcamp et al. (2010) with paleomagnetic data. Possible lateral blocks may still be seen on the north–east side of the Güimar collapse, and it is possible that the Micheque has not fully evacuated the scar, but remains partially as a landslide slump. The different intrusive densities and rates for the Micheque and Güimar collapses could link with different sliding rates.

Comparison with other oceanic volcanoes

A creeping spreading sector involves extension at the head of the slump area and strike-slip movement at the sides. This process has been evoked for Piton de La Fournaise, La Réunion Island by Bachelery (1981), Duffield et al. (1982), Merle and Lénat (2003) and Carter et al. (2007) (Fig. 9a). They observed, at the scale of the volcano, a series of slumps and related crescent-shaped rifts, with en échelon fissure eruptions and dykes. A similar pattern has developed on the Dolomieu cone (the central active vent) where strike-slip fractures and en échelon eruptive fissures are interpreted as the expression of progressive displacement of the area by

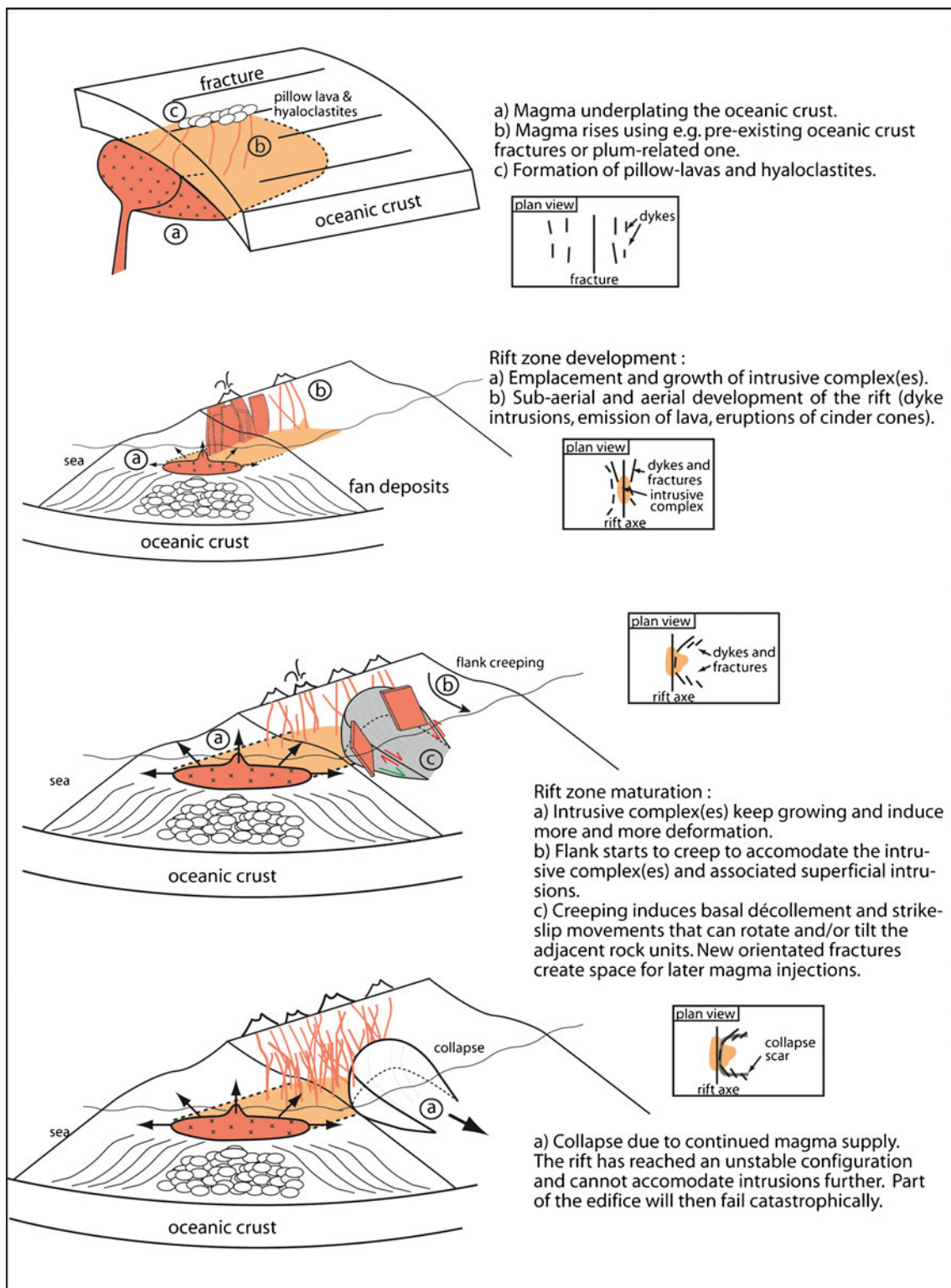


Fig. 8 Model cartoon of the development and growth of the NERZ that is largely controlled by the intrusive complex emplacement and its associated dykes. The model is divided into four main stages: (1) submarine stage with formation of pillow lavas and hyaloclastites; (2) rift zone sub-aerial and aerial development stage with the growth

of intrusive complex(es), the emplacement of dykes and lava flows and the eruption of cinder cones; (3) rift zone maturation stage where the mechanism of flank creeping is initiated; (4) if intrusive growth persists, the final stage will result in a catastrophic lateral collapse

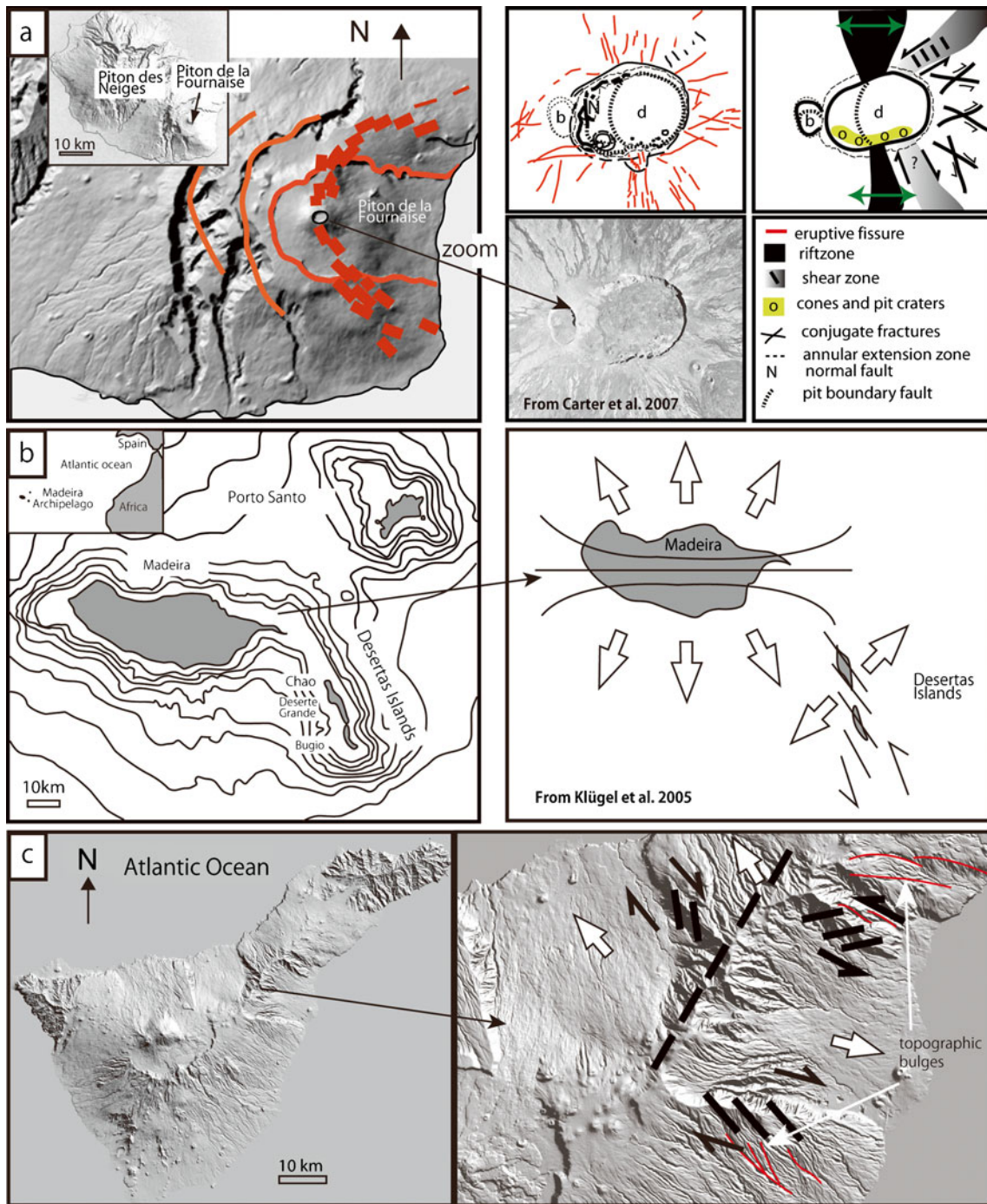


Fig. 9 Comparisons between several oceanic rift systems. **a** Piton de La Fournaise on La Réunion Island; the orientation of the rift zones, the fractures (in red) and the strike-slip fractures around the crater rim are interpreted as the results of flank spreading (figure from Carter et

al. 2007). **b** Bory Crater, **d** Dolomieu crater. **b** Strike-slip movements and dyke rotation at the Desertas Islands induced by spreading of Madeira (modified from Klügel et al. 2005). **c** Main dyke trends observed in the NERZ

flank spreading (Carter et al. 2007). Similarly, Klügel et al. (2005) note a deviation of the Desertas Islands dyke swarm in the Madeira Archipelago as a result of a spreading of Madeira that is accommodated by strike-slip movements (Fig. 9b). Such an arrangement of dyke trends is similar to the ones observed along the NERZ (Fig. 9c).

There are some barrancos along the NERZ flank that strike oblique to the scar walls (a few of them highlighted in red in Fig. 9c). We suggest that those parts are remnants of what sectors looked like before collapse. They indicate that the collapsed areas were topographic highs or at least surrounded by higher topography. Such

topographic bulges were probably the surface expression of intrusive complex growth, deformation and slumping, and these barrancos might be a morphological expression of the strike-slip fractures that accommodated the growth and emplacement of intrusive complex and dykes.

Following the major collapse events on the NERZ, the intrusive and eruptive rates were relatively low (Carracedo 1999), and La Orotava and Güímar embayments were so far only partially filled. Piton de la Fournaise on La Réunion Island is considerably more active. There, the intense intrusive activity is accommodated by periodic flank spreading of the Enclos Fouqué and adjacent areas, while older collapse features are partially buried, e.g. Merle et al. (2010). The growth of intrusive complexes in Piton de La Fournaise may also play a role, though unlike the NERZ, the loci of intrusion is nearly a point, so the complexes are likely to grow next to each other or to belong to just one long-lived feature. Gailler et al. (2009) note the presence of high gravity at the back of the Enclos Fouqué, which may be related to a former intrusive complex. Famin and Michon (2010) note the presence of outward dipping dykes, oblique to postulated collapse sides in Piton des Neiges, and Fukushima et al. (2005) also model oblique and seaward-dipping dykes in recent events for Piton de La Fournaise. These features are consistent with the NERZ model for prolonged creeping and intrusive activity before collapse.

On Hawaii, intrusive activity is also accommodated by flank displacement, but eruptive rates are very high and the collapse expressions are quickly covered by more recent eruptive products (Swanson et al. 1976; Dieterich 1988; Cayol et al. 2000; Brooks et al. 2008). The Micheque slide may be regarded as an analogue to the Hawaiian case, as the collapse embayment was rapidly filled by subsequent volcanism.

Conclusions

Our field data from Tenerife confirm that oceanic island rifts can be rather diffuse and have changeable geometry. Rifts grow during intense intrusive events, separated by periods of quiescence, deformation, erosion and collapse. Dykes vary in strike and dip at both outcrop and volcano flank scale. Furthermore, they predate and are oblique to the collapse scar walls, which contrasts with other models where dykes are parallel to and post-date the collapse scar. We interpret the dyke patterns and structures of the NERZ as evidence for flank creep. Forceful dyke emplacement centred around a developing intrusive complex favours sector spreading of the ridge, resulting in flank spreading on discrete sectors. This mechanism involves progressive displacements accommodated by extension and strike-slip movement at the head and along the walls of the deforming sector, respectively. Flank

slumping involves a basal detachment that appears to control the NERZ dyke dips and lateral strike-slip zones that control the NERZ dyke strikes. Flank spreading helps to stabilise the rift for some time, by reducing slopes. Progressive intrusive events and intrusive complex growth will cause deformation that will continue to steepen, brecciate and eventually destabilise the flank, triggering collapse event(s). Consequently, flank slumping constitutes a major mechanism for initial rift stabilisation, but may be insufficient to compensate for periods of high intrusive activity. In the NERZ, the two first collapses are thought to be essentially intrusion-driven (Micheque and Guímar), while the last one (La Orotava) is mainly gravity-controlled.

Acknowledgements L. Mathieu and S. Wiesmaier are thanked for their help in the field. R. Paris provided us with the DEM of Tenerife. D. Chew, A. Tibaldi, V. Acocella, P. Einarsson and two anonymous reviewers are greatly thanked for their comments and suggestions on earlier versions of the manuscript. This work was jointly funded by a National Geographic Society Grant in aid of research award 8106-06 (Petronis and Troll), by an Irish Research Council for Sciences, Engineering and Technology Grant (Delcamp and Troll) and by a Spanish Plan Nacional de I + D + I research project CGL2008-02842/BTE (Carracedo and Pérez-Torrado).

References

- Acocella V, Neri M (2009) Dike propagation in volcanic edifices: overview and possible developments. *Tectonophysics* 471:67–77
- Acocella V, Tibaldi A (2005) Dike propagation driven by volcano collapse: a general model tested at Stromboli, Italy. *Geophys Res Lett* 32:L08308. doi:10.1029/2004GL022248
- Allmendinger RW, Cardozo NC, Fisher D (2012) Structural geology algorithms: vectors & tensors. Cambridge University Press, England, p 289
- Ancochea E, Fuster JM, Ibarrola E, Cendrero A, Coello J, Hernan F, Cantagrel JM, Jamond C (1990) Volcanic evolution of the island of Tenerife (Canary Islands) in the light of new K-Ar data. *J Volc Geotherm Res* 4:231–249
- Anguita F, Hernán F (1975) A propagating fracture model versus a hot-spot origin for the Canary Islands. *Earth Planet Sci Lett* 27:11–19
- Araña V, Ortiz R (1986) Marco geodinámico del volcanismo canario. *An Física Vol Esp* 82:202–231
- Araña V, Ortiz R (1991) The Canary Islands: tectonics, magmatism and geodynamic framework. In: Kampunzu AB, Lubala RT (eds) *Magmatism in extensional structural settings—the Phanerozoic African Plate*. Springer, New York, pp 209–249
- Bachelery P (1981) Le Piton de la Fournaise (Ile de la Réunion): étude volcanologique, structurale et pétrologique. Ph.D. thesis, Université Blaise Pascal, Clermont-Ferrand
- Beck RH, Lehnert P (1974) Oceans, new frontiers in exploration. *Am Ass Petro Geol Bull* 58:376–395
- Bonali FL, Corazzato C, Tibaldi A (2011) Identifying rift zones on volcanoes: an example from La Réunion island. *Indian Ocean* 73:347–366. doi:10.1007/s00445-010-0416-1
- Borgia A (1994) Dynamic basis of volcano spreading. *J Geophys Res* 99:17791–17804
- Brooks BA, Foster J, Sandwell D, Wolfe CJ, Okubo P, Poland M, Myer D (2008) Magmatically triggered slow slip at Kilauea Volcano, Hawaii. *Science* 321(5893):1177

- Canales JP, Dañoibeitia JJ, Watts AB (2000) Wide-angle seismic constraints on the internal structure of Tenerife, Canary Islands. *J Volcanol Geotherm Res* 103:65–81
- Carracedo JC (1994) The Canary Islands; an example of structural control on the growth of large oceanic-island volcanoes. *J Volc Geotherm Res* 60:225–241
- Carracedo JC (1996) Morphological and structural evolution of the western Canary Islands: hotspot induced three-armed rifts or regional tectonic trends? *J Volcanol Geotherm Res* 72:151–162
- Carracedo JC (1999) Growth, structure, instability and collapse of Canarian volcanoes and comparisons with Hawaiian volcanoes. *J Volcanol Geotherm Res* 94:1–19
- Carracedo JC, Rodríguez Badiola E, Guillou H, Pateme M, Scaillet S, Pérez Torrado FJ, Paris R, Fra-Paleo U, Hansen A (2007) Eruptive and structural history of Teide Volcano and rift zones of Tenerife, Canary Islands. *GSA Bull* 19:1027–1051. doi:10.1130/B26087.1
- Carracedo JC, Guillou H, Nomade S, Rodríguez-Badiola E, Pérez-Torrado FJ, Rodríguez-González A, Paris R, Troll VR, Wiesmaier S, Delcamp A, Fernández-Turiel JL (2010a) Evolution of ocean island rifts: the Northeast rift zone of Tenerife, Canary Islands. *Geol Soc Am Bull* B30119.1. doi:10.1130/B30119.1
- Carracedo JC, Fernández-Turiel JL, Gimeno D, Guillou H, Klügel A, Krastel S, Paris R, Pérez-Torrado FJ, Rodríguez-Badiola E, Rodríguez-González A, Troll VR, Walter TR, Wiesmaier S (2010b) Comment on “The distribution of basaltic volcanism on Tenerife, Canary Islands: implications on the origin and dynamics of the rift systems” by A. Geyer and J. Martí. *Tectonophysics* 483:310–326
- Carter A, van Wyk de Vries B, Kelfoun K, Bachèlery P, Briole P (2007) Pits, rifts and slumps: the summit structure of Piton de la Fournaise. *Bull Volcanol* 69:741–756. doi:10.1007/s00445-006-0103-4
- Cayol V, Dieterich JH, Okamura AT, Miklius A (2000) High magma storage rates before the 1983 eruption of Kilauea, Hawaii. *Science* 288:2343. doi:10.1126/science.288.5475.2343
- Clemente CS, Amorós EB, Crespo MG (2007) Dike intrusion under shear stress: effects on magnetic and vesicle fabrics in dikes from rift zones of Tenerife (Canary Islands). *J Struct Geol* 29:1931–1942
- Deegan FM (2010) Processes of magma–crust interaction: insights from geochemistry and experimental petrology. Ph.D. thesis, Uppsala University, Sweden. Comprehensive summary available at <http://uu.diva-portal.org/smash/get/diva2:358897/FULLTEXT01>
- Delaney P, Pollard DD (1981) Deformation of host rocks and flow of magma during growth of Minette dikes and breccia-bearing intrusions near Ship Rock, New Mexico. *US Geol Surv Prof Pap* 1202, 61 pp
- Delcamp A (2010) Evolution of the NE rift-zone of Tenerife, Canary Islands: a multi-disciplinary approach. Ph.D. thesis, Trinity College Dublin, Ireland
- Delcamp A, van Wyk de Vries B, Troll VR (2007) Endogeneous and exogeneous evolution of a cinder cone: example of Lemptégy cinder cone, Auvergne, France. *EGU A-04948*, Vienna, Austria
- Delcamp A, Petronis MS, Troll VR, Carracedo JC, van Wyk de Vries B, Perez-Torrado FJ (2010) Vertical axis rotation of the upper portions of the north-east rift of Tenerife Island inferred from paleomagnetic data. *Tectonophysics* 492:40–59
- Delcamp A, van Wyk de Vries B, James MR, Gailler LS, Lebas E (2011) Relationships between volcano gravitational spreading and magma intrusion. *Bull Volcanol*. doi:10.1007/s00445-011-0558-9
- Dieterich JH (1988) Growth and persistence of Hawaiian volcanic rift zones. *J Geophys Res* 93:4258–4270
- Duffield W, Stieltjes L, Varet J (1982) Huge landslide blocks in the growth of Piton de la Fournaise, La Reunion and Kilauea Volcano, Hawaii. *J Volcanol Geotherm Res* 12:147–160
- Elsworth D, Day SJ (1999) Flank collapse triggered by intrusion: the Canarian and Cape Verde Archipelagoes. *J Volcanol Geotherm Res* 94:323–340
- Elsworth D, Voight B (1996) Evaluation of volcano flank instability triggered by dyke intrusion. *Geol Soc Spec Publ* 110:45–53
- Famin V, Michon L (2010) Volcano destabilization by magma injections in a detachment. *Geology* 38:219–222
- Fiske R, Jackson ED (1972) Orientation and growth of Hawaiian volcanic rifts: the effect of regional structure and gravitational stresses. *Proc R Soc Lond Ser A* 329:299–326
- Fukushima Y, Cayol V, Durand P (2005) Finding realistic dike models from interferometric synthetic aperture radar data: the February 2000 eruption of Piton de la Fournaise. *J Geophys Res* 110. doi:10.1029/2004JB003268
- Fúster JM, Araña V, Brandle JL, Navarro JM, Alonso U, Aparicio A (1968) *Geología y Volcanología de las Islas Canarias: Tenerife*. Inst Lucas Mallada, CSIC, Madrid, pp 1–218
- Gailler LS, Lénat JF, Lambert M, Levieux G, Villeneuve N, Froger JL (2009) Gravity structure of Piton de la Fournaise volcano and inferred mass transfer during the 2007 crisis. *J Volcanol Geotherm Res* 184:31–48
- Geyer A, Martí J (2010) The distribution of basaltic volcanism on Tenerife, Canary Islands: implications on the origin and dynamics of the rift systems. *Tectonophysics* 483:310–326
- Gudmundsson A (2000) Dynamics of volcanic systems in Iceland: example of tectonism and volcanism at juxtaposed hot spot and mid-ocean ridge systems. *Ann Rev Earth Planet Sci* 28:107–140
- Gudmundsson A (2002) Emplacement and arrest of sheets and dykes in central volcanoes. *J Volcanol Geotherm Res* 116:279–298
- Gudmundsson A, Marinoni LB, Martí J (1999) Injection and arrest of dykes: implications for volcanic hazards. *J Volcanol Geotherm Res* 88:1–13
- Guillou H, Carracedo JC, Paris R, Pérez Torrado FJ (2004) Implications for the early shield-stage evolution of Tenerife from K/Ar ages and magnetic stratigraphy. *Earth Planet Sci Lett* 222:599–614
- Hildenbrand A, Gillot P-Y, Le Roy I (2004) Volcano-tectonic and geochemical evolution of an oceanic intra-plate volcano: Tahiti-Nui (French Polynesia). *Earth Planet Sci Lett* 217:349–365
- Hoek JD (1995) Dyke propagation and arrest in Proterozoic tholeiitic dyke swarms, Vestfold Hills, East Antarctica. In: Baer G, Heimann A (eds) *Physics and chemistry of dykes*. Balkema, Rotterdam, pp 79–93
- Klügel A, Walter TR, Schwarz S, Geldmacher J (2005) Gravitational spreading causes en-echelon diking along a rift zone of Madeira Archipelago: an experimental approach and implications for magma transport. *Bull Volcanol* 68:37–46
- Le Maitre RW, Bateman P, Dudek A, Keller J, Lameyre J, Le Bas MJ, Sabine PA, Schmid R, Sorensen H, Streckeisen A, Woolley AR, Zanettin B (1989) *A classification of igneous rocks and glossary of terms: recommendations of the International Union of Geological Sciences Subcommittee on the Systematics of Igneous Rocks*. Blackwell Scientific, Oxford
- Longpré MA, Troll VR, Hansteen TH (2008) Upper mantle magma storage and transport under a Canarian shield-volcano, Teno, Tenerife (Spain). *J Geophys Res* 113:B08203. doi:10.1029/2007JB005422
- Márquez A, López I, Herrera R, Martín-González F, Izquierdo T, Carreño F (2008) Spreading and potential instability of Teide volcano, Tenerife, Canary Islands. *Geophys Res Lett* 35: L05305. doi:10.1029/2007GL032625
- Martí J, Gudmundsson A (2000) The Las Cañadas caldera (Tenerife, Canary Islands): an overlapping collapse caldera generated by magma-chamber migration. *J Volcanol Geotherm Res* 103:161–173
- Martí J, Mitjavila J, Araña V (1994) Stratigraphy, structure and geochronology of the Las Cañadas caldera (Tenerife, Canary Islands). *Geol Mag* 131:715–727
- Martí J, Hurlimann M, Ablay GJ, Gudmundsson A (1997) Vertical and lateral collapses on Tenerife (Canary Islands) and other volcanic ocean islands. *Geology* 25:879–882

- Mathieu L, van Wyk de Vries B (2009) Edifice and substrata deformation induced by intrusive complexes and gravitational loading in the Mull volcano (Scotland). *Bull Volcanol* 71:1133–1148
- McFarlane DJ, Ridley WI (1968) An interpretation of gravity data for Tenerife, Canary Islands. *Earth Planet Sci Lett* 4:481–486
- McGuire WJ, Pullen AD (1989) Location and orientation of eruptive fissures and feeder dykes at Mount Etna; influence of gravitational and regional stress regimes. *J Volcanol Geotherm Res* 38:325–344
- Merle O, Lénat JF (2003) Hybrid collapse mechanism at Piton de la Fournaise (Réunion Island, Indian Ocean). *J Geophys Res* 108:2166
- Merle O, Mairine P, Michon L, Bachèlery P, Smietana M (2010) Calderas, landslides and paleo-canyons on Piton de la Fournaise volcano (La Réunion Island, Indian Ocean). *J Volcanol Geotherm Res* 189:131–142
- Oehler JF, van Wyk de Vries B, Labazuy P (2005) Landslides and spreading of oceanic hot-spot and arc shield volcanoes on Low Strength Layers (LSLs): an analogue modeling approach. *J Volcanol Geotherm Res* 144:169–189
- Porreca M, Acocella V, Massimi E, Mattei M, Funicello R, De Benedetti AA (2006) Geometric and kinematic features of the dike complex at Mt. Somma, Vesuvio (Italy). *Earth Planet Sci Lett* 245:389–407
- Robertson AHF, Stillman CJ (1979) Submarine volcanic and associated sedimentary rocks of the Fuerteventura Basal Complex, Canary Islands. *Geol Mag* 116:203–214
- Rodríguez-Losada JA, Hernández-Gutiérrez LE, Olalla C, Perucho A, Serrano A, Eff-Darwich A (2009) Geomechanical parameters of intact rocks and rock masses from the Canary Islands: implications on their flank stability. *J Volcanol Geotherm Res* 182:67–75
- Swanson DA, Duffield WA, Fiske RS (1976) Displacement of the south flank of Kilauea Volcano: the result of forceful intrusion of magma into the rift zone. *US Geol Surv Prof Pap* 963:39
- Tibaldi A (2001) Multiple sector collapses at Stromboli volcano, Italy: how they work. *Bull Volcanol* 63:112–125
- Tibaldi A (2003) Influence of cone morphology on dykes, Stromboli, Italy. *J Volcanol Geotherm Res* 126:79–95
- van Bemmelen RW (1949) The geology of Indonesia: general geology of Indonesia and adjacent archipelagos. Gov. Print. Off, The Hague
- van Wyk de Vries B, Matela R (1998) Styles of volcano-induced deformation: numerical models of substratum flexure, spreading and extrusion. *J Volcanol Geotherm Res* 81:1–18
- van Wyk de Vries B, Cecchi E, Robineau B, Merle O, Batchèlery P (2001) Factors governing the volcano-tectonic evolution of La Réunion Island: a morphological, structural and laboratory modelling approach. *J Conf Abst* 6:800
- Walker GPL (1992) Coherent intrusion complexes in large basaltic volcanoes; a new structural model. *Essays on magmas and other earth fluids; a volume in appreciation of Harris PG, Cox KG, Baker PE.* Elsevier 50:41–54
- Walter TR, Troll VR (2003) Experiments on rift zone evolution in unstable volcanic edifices. *J Volcanol Geotherm Res* 127:107–120
- Walter TR, Troll VR, Cailleau B, Belousov A, Schmincke HU, Bogaard P, Amelung F (2005) Rift zone reorganization through flank instability on ocean island volcanoes: Tenerife, Canary Islands. *Bull Volcanol* 67:281–291
- Walter TR, Klügel A, Münn S (2006) Gravitational spreading and formation of new rift zones on overlapping volcanoes. *Terra Nova* 18:26–33
- Watts AB (1994) Crustal structure, gravity anomalies and flexure of the lithosphere in the vicinity of the Canary Islands. *Geophys Int* 119:648–666
- Watts AB, Masson DG (1995) A giant landslide on the north flank of Tenerife, Canary Islands. *J Geophys Res* 100:24487–24498